Journal of Materials Chemistry A

Accepted Manuscript

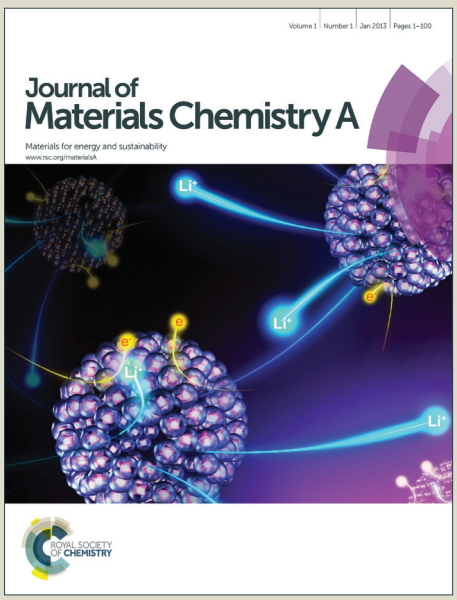

ROYAL SOCIETY OF CHEMISTRY

www.rsc.org/materialsA

First principles guide to tune *h-BN* nanostructures as superior light element based hydrogen storage material: Role of bond exchange spillover mechanism

E. Mathan Kumar, S. Sinthika and Ranjit Thapa*

SRM Research Institute, SRM University, Kattankulathur - 603203, Tamil Nadu, India.

*Corresponding Author

E-mail: ranjit.t@res.srmuniv.ac.in, Tel. No.: +91-44-27417918, Fax: +91-44-27456702

ABSTRACT

We investigate the interaction of molecular hydrogen with light element based *n*-doped hexagonal boron nitride (*h-BN*) nanostructures and moreover explore the bond exchange mechanism for spillover of atomic hydrogen using dispersion-corrected density functional theory (DFT-D) calculations. A number of doped configurations were tested and it has been found that co-doping of C and O on *h-BN* sheet significantly increases the adsorption energy of molecular H_2. The charge transfer from the *n*-doped *h-BN* surface to H_2 is found to be the reason for the higher interactions that boosted the binding energy. In addition, the doped *h-BN* surfaces act as catalysts and dissociate the H_2 molecule with very low activation barrier, but the migration of the resulting H atoms on the surface requires high energy. In order to facilitate easy and fast migration of H atoms, we introduce the bond exchange mechanism using external mediators i.e. borane (BH_3) and gallane (GaH_3) molecules which serve as a secondary catalysts and help in lowering the migration barrier, leading to the formation of hydrogenated surface. The partially hydrogenated surface in turn can also act as a hydrogen storage material, with a higher propensity to adsorb hydrogen molecules when compared to the unhydrogenated surface. Hence the surface proposed in this work can be used to store substantial quantity of hydrogen as energy source with easy adsorption and desorption kinetics.

Keywords: Adsorption, Hydrogenation, Density functional theory, Doping, Catalyst

1 Introduction

Hydrogen as energy source can be stored mainly in two forms, one as hydrogen molecule (H_2) adsorbed weakly on various surfaces (mainly physical adsorption)[1-3] and another as atomic hydrogen (H) bonded strongly with other elements (chemical bonding).[4-6] H_2 storage via physical adsorption is fully reversible and follow fast kinetics in comparison to the chemically bonded H atom, which usually needs high release temperatures. As per the concern of reversibility and stability, the H_2 binding energy should be in certain energy window i.e. about 0.2-0.7 eV.[7] From various studies it has been observed that the adsorption energy of H_2 on transition metal (TM) clusters supported on graphene and other 1D/2D nanostructure is in the desirable range.[8-13] But the major problem during hydrogen storage using metal adatoms/clusters via physical interaction is low gravimetric ratios at ambient conditions.[14,15] So to store the H_2 with high gravimetric density, the host material should only consist of light elements such as Be, B, C, O, N etc.[16-19] However storing of H_2 in the light element based materials with moderate binding energy remains a challenge. Overall, current research is mainly focused on designing efficient hydrogen storage materials to reach the department of energy (DOE) targets viz. gravimetic density of 9.0 wt %, volumetric density of 81g/L, operating temperature in the range of -40 to 85^0C and applied pressure in the range of 1-100 atm.

There are several motivating works on carbon based nanomaterials (such as carbon nanotube (CNT), graphene, and fullerene) and metal organic frameworks (MOF) that illustrate them as possible materials for hydrogen storage.[20-24] Recently Chen *et al.* reported that Mg doped graphene oxide (GO) enhances the storage capacity upto 5.6 wt % at a temperature of about 200 K. The binding energy of H_2 with GO is found to be mainly dependent on the polarization interaction between Mg and O.[22] Another study signifies that boron doped graphene is a good medium for hydrogen storage when decorated with alkaline

earth metals (AEM) like Mg and Ca. The H_2 interaction on this medium shows a crossover between Kubas and multipole Coulomb effect depending on the ionic state of AEM and the number of adsorbed H_2 molecules.[23] Durgun *et al.* have found that substitutional doping of Be into single wall carbon nanotube (SWNT) improves the H_2 binding energy up to 0.40 eV, which is very high compared to the pure SWNT (60 meV). The charge transfer from Be (~ 1.2 *e*) to nearest carbon atoms (~ 0.4 *e* to each neighbors) is established to be the cause of the enhanced binding strength.[24] Hexagonal boron nitride (*h-BN*) nanostructures also originate as good medium for hydrogen storage, when their electronic structure is perturbed.[25-27] For instance, carbon doped boron nitride cages are proven to have promising potential as hydrogen storage materials with a storage capacity of 7.43 wt %. The activation energy for hydrogenation and dehydrogenation from $B_{11}N_{12}C$ surface is found to be about 2 eV at room temperature and 10 bar applied pressure, with the repulsion between the electrons of the hydrogen and π electron of $B_{11}N_{12}C$ reducing the energy barrier for dehydrogenation.[28] Also it has been reported that Li decorated boron nitride atomic chain (BNAC) show a high storage capacity of 25.4 wt % because of strong hybridization between lithium 2*p* orbital and nitrogen 2*p* orbital along with the polarization interaction between H_2 molecule and Li decorated BNAC.[29] On the other hand Han *et al.*[30] explained that the spillover mechanism using a secondary catalyst can help in the formation of partially hydrogenated graphene surface with very low barrier energy and the number of atomic hydrogen bound to the substrate is a predominant factor to tune the magnitude of H_2 binding energy value.

In this work, we extensively study the H_2 interaction with pure and C, O, 2C, C-O and 2C-O doped *h-BN* monolayer and boron nitride nanocage ($B_{12}N_{12}$). Our calculations reveal that among the entire doping configuration, C-O doping synergistically enhances the chemical activity of *h-BN* nanostructures, leading to a higher value of adsorption energy. The

donation of electrons from p_z (of doped surface) to $1\sigma^*$ orbital of H_2 is assigned to be the cause of high binding energy as compared to pure *h-BN* case. We found that there is a probability of H_2 dissociation on doped *h-BN* surface with low activation energy barrier. However, the migration of the dissociated hydrogen atom along the doped and pure *h-BN* surfaces is unfavorable. We propose that secondary mediators such as *borane (BH_3)* and *gallane (GaH_3)* can help in the migration of H atom along the surface with very low barrier energy via bond exchange spillover mechanism. So during the H_2 adsorption and desorption process a partially hydrogenated surface is possible to form. Interestingly, it has been found that this partially hydrogenated *h-BN* monolayer has the tendency to bind H_2 molecule with higher binding energy value, and also could be considered as a H_2 storage surface.

2 Computational Details

We performed the calculations using spin polarized density-functional theory as implemented in the Cambridge Serial Total Energy package (CASTEP).[31] The Vienna ab-Initio simulation package (VASP) has also been used for further verification.[32] The generalized gradient approximation (GGA) was employed for exchange and correlation effect at Perdew-Burke-Ernzerhof (PBE)[33] and Perdew and Wang's 1991 (PW91) level.[34] The potentials of the atoms were described by the ultrasoft pseudopotentials approach[35] and projected augmented wave (PAW) method.[36] The plane-wave basis set was considered with energy cutoff of 400 eV. Brillouin zone sampling was made with the Monkhorst Pack scheme and a K-Point grid of 7x7x1. For long-range van der Waals interaction, the parameter-free Tkatchenko−Scheffler (TS)[37] and Ortmann Bechstedt and Schmidt (OBS) method[38] were used with PBE and PW91 functional respectively (denoted as PBE+D or PBE+TS and PW91+D or PW91+OBS from here). All the structures were optimized until the total energy converged to less than 10^{-5}eV/atom and the maximum force converged to lower than 0.01

eV/Å. The complete linear and quadratic synchronous transit method (LST/QST) implemented in CASTEP was used to search for the Transition states.[39] The nudged elastic band (NEB) method was also employed to estimate the transition states for further verification. We used (4×4) and (5×5) supercells (along a and b axis) and 20 Å vacuum along c-axis as the model geometry to explain our results. The binding energy ($E_{B.E}$) between the H_2 molecule and the doped surface is defined as

$$E_{B.E} = E(\text{doped } h\text{-}BN + nH_2) - E[\text{doped } h\text{-}BN + (n\text{-}1)\ H_2] - E\ (H_2), \quad (1)$$

where E(doped *h-BN* + nH_2) is the total energy of the doped BN system with nH_2 molecules adsorbed, E [doped *h-BN*+ (n-1) H_2] is the energy of the same system with (n-1) H_2 molecules adsorbed and E (H_2) is the total energy of an isolated H_2 molecule.

3. Results and Discussions

3.1 Single H_2 adsorption

Hexagonal boron nitride monolayer and $B_{12}N_{12}$ nanocage were chemically modified by substitutionally doping with carbon and oxygen atom. We substitute the C and O atom for B and N in *h-BN* surfaces correspondingly (an example of *n*-doped system). As the formation energy of an O atom replacing a B atom of *h-BN* is very high, this structure is predicted to be highly unstable[40], and hence we did not investigate this case. In Table S1 and Fig. S1 of supplementary information (SI), the formation energies of different configurations of doped *h-BN* sheet are summarized. Moreover, we have reported that doping enhances the activity of the *h-BN* monolayer.[41] In order to test the storing capacity of hydrogen molecule on this class of surfaces, we first made a single H_2 molecule to interact with monolayer of doped *h-BN* and $B_{12}N_{12}$ nanocage. Since the interaction energy of nonpolar H_2 molecules with the substrates containing light elements is mainly in the physisorption (London dispersion) range,[42] we

consider the van der Waals interaction corrected total energy term to get more accurate results. We mainly use PBE+D and PW91+D approach to serve this purpose.[43]

The optimized structures of a single H_2 molecule adsorbed on various doped *h-BN* monolayer are shown in Fig. 1. The H_2 binding energies and H_2-surface distances (d_a) are shown in the inset of each subfigure of Fig. 1. First, we examined the role of adsorption site of different doped *h-BN* surfaces. Mainly four different sites were tested, the top site of C, O, N and B atoms. We confirm that for doped systems, B and C atoms anchor the H_2 molecule with a slightly higher binding energy as compared to O and N atoms, as shown in the Fig. 1 and Fig. S2 of the SI. The adsorbed geometry of a H_2 molecule on C doped *h-BN* (CBN) is shown in Fig. 1a. Using the PW91+D functional the binding energy value is found to be about -0.16 eV, which is higher than the value obtained using PBE+D functional ($E_{B.E}$ = -0.06 eV). Next we have taken into account the oxygen doped *h-BN* (OBN) surface, shown in Fig. 1b for H_2 adsorption. A similar trend has been observed in this surface, the PW91+D functional showing a higher binding energy value compared to PBE+D functional. The higher binding energy of H_2 on OBN ($E_{B.E}$ = -0.18 eV using PW91+D) as compared to the CBN surface indicates that O doping enhances the interaction energy of *h-BN* system to capture H_2 molecules, which has been also experimentally observed by *Lei et al*[44]. This may be attributed to the fact that, upon doping with oxygen, the *h-BN* surface undergoes structural modification and unequal amounts of charge are imparted to the surrounding boron atoms,[41] which causes the B atom adjacent to the O dopant to become highly active. Next we assessed the H_2 adsorption ability of co-doped (C and O both) *h-BN* monolayer (COBN)[40]. We choose the para configuration of C and O co-doped *h-BN* surface based on lowest formation energy (please see Fig. S1 in the SI). The H_2 adsorption is even stronger in the COBN surface, with $E_{B.E}$ = -0.28 eV (optimized structure is shown in Fig. 1c) and is higher than the other surfaces. In this case the H_2-surface distance is about 2.58 Å. For this system the binding

energy value is larger than the required chemical potential of H_2 to store at 30 ^{0}C and 100 bar pressure.[30] Next we increase the number of C dopants to two (2CBN) (optimized structure shown in Fig. 1d). The binding energy of H_2 on this system is higher than single-atom doping, but is less than the OBN and COBN systems. In order to increase the hydrogen storage ability of this surface, we doped an O atom onto the 2CBN system (2COBN) (Fig. S3). Our results reveal that the binding energy of H_2 on 2CO doped *h-BN* surface is higher than C, O and 2C doped *h-BN* system, but is still lesser than that of COBN system. These results indicate that the COBN structure is highly efficient in storing the hydrogen molecule as compared to all other doping configurations studied.

In order to find out the role of functionals on the H_2-surface interaction energy value, single hydrogen molecule binding energies are calculated for all type of configurations using PBE, PBE+TS, PW91, PW91+OBS, PBE_{sol} functionals and are tabulated in Table 1. Examination of Table 1 reveals that the binding energy values estimated using PW91 functional are mostly negative and higher than the $E_{B.E}$ using PBE functional. In these surfaces the PBE functional underestimates the binding energy values, agreeing well with the reported results of *Wang et. al.*[29] Also *Sun et. al.*[45] accentuate that PW91 functional can estimate the proper binding energy in case of hydrogen adsorption. Similarly considering the dispersion energy term it has been found that the magnitude of binding energies are higher for the PW91+OBS compared to PBE+TS functional. Both the functionals follow the same trend in binding energy for different surfaces. It can be interpreted that PW91+OBS functional treats van der Waals force more correctly in these cases.[46] So we used PW91+OBS functional for the further studies and the functional-dependent binding energy of H_2 on various doped *h-BN* configurations have been elaborately discussed in the later section. From the Table 1, it can also be inferred that the H_2 adsorption is highly preferred on COBN and

2COBN systems (in view of all functionals), suggesting these surfaces to be efficient materials for hydrogen storage.

Now we consider one more example of BN surface (BN-nanocage, $B_{12}N_{12}$) for finding the trend of H_2 binding energy value as a function of dopants. The $B_{12}N_{12}$ is recognized to be a stable form of boron nitride[28], and its high surface to volume ratio can be employed to store larger number of hydrogen molecules. Similar to the monolayer case, the BN-nanocage was doped with C and O atoms, and the optimized structures are shown in Fig. 2. Binding energy of single H_2 adsorption on C doped BN-nanocage ($CB_{11}N_{12}$, we consider the similar notation from here for all the cases) is $E_{B.E}$ = -0.12 eV (see Fig. 2a) (the value is similar to the previous work[28]). In case of $OB_{12}N_{11}$ the $E_{B.E}$ = -0.14 eV, the increment in binding energy can be attributed to the fact that, O doping on $B_{12}N_{12}$ leads to slight structural distortion of the host material, thereby increasing its ability to adsorb hydrogen molecules (see Fig. 2b). C-O co-doped on BN-nanocage ($COB_{11}N_{11}$) is shown in Fig. 2c, here the $E_{B.E}$ = -0.15 eV, which is very low compared to COBN but is slightly higher than $OB_{12}N_{11}$ and $CB_{11}N_{12}$ and the distance between H_2 and the surface is about 2.83 Å. Using the enthalpy ΔH (i.e binding energy), the estimated free energy change (ΔG) during hydrogenation (H_2 adsorption) on ($COB_{11}N_{11}$) surface at room temperature and 10 bar pressure shows better storage medium compare to the ($CB_{11}N_{12}$) surface.[28] If we increase the number of carbon dopants to two in the BN-nanocage ($2CB_{10}N_{12}$), the binding energy is found to be -0.13 eV, the structure is shown in Fig. 2d. The $CB_{11}N_{12}$ and $2CB_{10}N_{12}$ doping configurations of the nanocages exhibit similar adsorption energy values because of low charge transfer from doped surface to H_2 molecule. In order to promote the interaction of H_2 with the cages, we doped one more oxygen into 2CBNcage ($2COB_{10}N_{11}$) and the binding energy increases to -0.16 eV with optimized d_a = 2.410 Å (see Fig. S4). $2COB_{10}N_{11}$ can be regarded as the best

storage medium among the doped BN cages considered here as its interaction with H_2 surpasses the others.

3.2 Multi H_2 adsorption

Next we systematically investigated the interaction of more than one H_2 molecule on the various doped *h-BN* monolayer (COBN, 2CBN, 2COBN). We used the PW91+D functional for this purpose as it provides consistent energy values, described earlier in the text. In Fig. 3, the binding energy is presented as a function of the number of the adsorbed H_2 molecules. We added H_2 molecules to the surface one by one, relaxing the structure each time (taking into account that H_2 molecules adsorb on the surface one by one, during storage). Since lateral interactions between H_2 molecules may contribute significantly to the binding energy (discussed in detail in later section), we placed the H_2 molecules at a distance of ~ 3 Å from each other to ensure that H_2-H_2 interactions are minimal. The optimized structure of two hydrogen molecules on the COBN surface is shown in Fig. 3a. Here the binding energy per H_2 on the COBN surface is about -0.23 eV, which is comparatively smaller than the single H_2 adsorbed on the COBN surface. Three H_2 molecules adsorbed on the COBN surface is shown in Fig. 3b, here the estimated $E_{B.E}$ per H_2 is about -0.25 eV, which is slightly higher than the case of two H_2 adsorbed on the COBN surface. Now on addition of the fourth H_2 molecule on COBN (see Fig. 3c) the $E_{B.E}$ per H_2 increases to about -0.28 eV. Trends in the estimated results indicate that for COBN surface the binding energy per H_2 increases with the total number of H_2 molecules per supercell, which is contrary to the case of metal-based systems wherein the binding energy per H_2 decreases with number of H_2 molecules.[29, 47] We also note that the bond length of free H_2 molecule is d_b = 0.75 Å which is elongated to 0.78 Å in case of H_2 (first molecule) adsorbed on COBN system. Next, all the B and C sites of the COBN surface (only considered the single side of the COBN surface) were covered with H_2 molecules ($16H_2$) in order to assess the ultimate binding energy limit. In fact, our results

reveal that the binding energy per H_2 molecule for $16H_2$ molecules adsorbed on COBN surface increases to -0.42 eV. This increase of binding energy behavior clearly indicates that COBN surface is a good medium for H_2 uptake at ambient conditions. In the same way, we follow the multi hydrogen molecule adsorption on 2CBN and 2COBN surfaces and plotted the binding energy of all these configurations as a function of number of H_2 molecules as shown in Fig. 3d. The trend of binding energy obtained is similar for all the configurations. We need additional studies to understand the nature of interaction among the H_2 molecules and the surface. Also it has to be noted that increasing C-O co-doping concentration (ex: 2C2O, 3C3O per unit supercell are considered here) enhances the binding energy of H_2 molecule, which is an obvious phenomena and also a simple way to tune the binding energy(for more details see Fig. S5).

3.3 Interaction I: Partial density of states (PDOS)

In order to gain a deeper insight into the cause of binding between the H_2 molecule and the COBN monolayer, we plot the spin polarized partial density of states (PDOS) of (one, two, three and sixteen) H_2 adsorbed COBN systems, shown in Fig. 4. Here we consider the density of states only for C, O and B atoms (nearest to the H_2 molecule) for simplicity (indicated by the solid line), and PDOS of the H_2 molecules are depicted using a filled area plot, for easier interpretation. The donor electronic state (of both minority and majority carriers) at about -0.8 eV below the Fermi level (E_f) of the COBN surface is a clear indication of two–electron doping. The non-magnetic ground state of C-O co-doped *h-BN* is more favorable as per the functional used in this case. Before adsorption, the $1\sigma^*$ orbital of free H_2 molecule is empty and lies above the Fermi level. From the PDOS for the single H_2 adsorbed on B site of COBN in Fig. 4a, it is clear that there is electron donation from the surface donor state to the $1\sigma^*$ orbital of the H_2 molecule, making it partially occupied. The inset shows a closer view of PDOS near the Fermi level. The hybridization of states between defect levels

and $1\sigma^*$ orbital of H_2 molecule can be inferred to be the cause of increased binding energy of surface-H_2 due to doping. Fig. 4 (b) (c) and (d) show the PDOS of two, three and sixteen H_2 molecules adsorbed on the same surface (COBN). The Fig. 4 clearly demonstrate that, relatively the partial occupancy of state of H_2 molecules below the Fermi level is increasing as compared to single H_2 case. This phenomenon explains why the binding energy per H_2 molecule on such surfaces remains similar even when the concentration of H_2 increases. Also it has to be noted that the partial occupancy of $1\sigma^*$ orbital of the H_2 molecule increases in case of higher percentage C-O co-doping on the surface.

3.4 Interaction II: Isosurface and electron density difference

In order to analyze the nature of interactions that contributes to the total energy of the system, we make two models: In the first case, H_2 molecules are adsorbed on four boron sites and are made to interact with each other with an average distance of 2 Å (henceforth named as $4H_2$-cluster) and in the second case, we remove a single H_2 molecule from the most active B site and place it far from the other $3H_2$ molecules at a distance of ~ 4Å (termed as farH_2-$3H_2$cluster). The binding energy per H_2 molecule was calculated for the two cases. The binding energy per H_2 molecule in case of $4H_2$-cluster is about -0.31 eV (the structure is shown in the Fig. 5a). For farH_2-$3H_2$ cluster case we found that the binding energy per H_2 decreases to about -0.22 eV (see Fig. 5b). This result clearly indicates that an active B site, near or far from C-O doping area plays a vital role in determining the adsorption energy of H_2. We believe that as H_2 clustering is more favorable in this case, the H_2-H_2 self-interaction also contributes to the enhancement in binding energy (discussed later). Now we examine the origin of larger binding of H_2, particularly with C-O co-doped *h-BN* monolayer and provide more insight into the cause of difference in binding energy of the H_2-cluster and the farH_2-$3H_2$ cluster with the surface, by performing isosurface and charge redistribution analysis. We

study mainly how the electronic charge density gets modified upon adsorption of H_2 molecule. More specifically, we plot isosurfaces using the equation

$$\Delta\rho = \rho\,(\text{COBN} + H_2) - \rho\,(\text{COBN}) - \rho\,(H_2) \qquad (2)$$

where the terms on the right-hand-side (from left) of the equation are the electronic charge densities of the combined system, the doped *h-BN* alone, and the hydrogen molecule alone respectively. In Fig. 5c & d, we have plotted the isosurfaces of $4H_2$-cluster and far H_2-$3H_2$ cluster adsorbed on COBN surface. The green lobes correspond to an accumulation of electrons, and the yellow lobes correspond to a depletion of electrons. The value we have chosen for plotting the isosurface is 2×10^{-3} e/bohr^3 for both the cases. The permanent dipole moment on the COBN substrate induces charge redistribution in the hydrogen molecules, which results in the formation of dipole moment in each H_2 molecule. This induced dipole on H_2 molecules signifies that it is the electrostatic interaction that binds the H_2 molecules to the COBN surface.[48] From Fig. 5c it is clear that the magnitude of the charge contained within the green lobe is higher than that of yellow lobe. The estimated results reveal that charge has been transferred from the surface to the H_2 molecules. Moreover, in the $4H_2$-cluster case a green lobe is formed (indicated with solid red circle in Fig. 5c) between H_2 molecule and the C site, which helps to increase the binding between the particular H_2 with the surface. Formation of this green lobe clearly indicates that the charge has been removed from the π orbital of carbon atom and is accumulated in the free region instead of any sites. It is also worth noting that the H_2 molecule indicated by the blue dotted circle in Fig. 5d (farH_2-$3H_2$cluster case) has a different orientation of the green and yellow lobes as compared to the other H_2 molecules .

Charge density differences were also calculated for the same two cases ($4H_2$-cluster and farH_2-$3H_2$cluster) and are shown in Fig. 5e & f, respectively. A planar slice considered

along the direction parallel to the COBN surface touches all the four H_2 molecules, which helps to understand the interaction between H_2-H_2 molecules (if any) and also with the surface. The electron enrichment is indicated by red color, loss of electrons is shown by blue color and white color indicates the region with very small change in the electron density. The dotted black circle around the H_2 molecule indicates a large gain of electronic charge from the COBN surface. This is consistent with the insight obtained from the PDOS and isosurface analysis of the previous sections. The H_2-H_2 self interaction is higher in the case of $4H_2$-cluster compared to the farH_2-$3H_2$ cluster, as can be inferred from the Fig. 5e and f. This clearly suggests that the self interaction energy also contributes to the binding energy value. For more insight we performed a test calculation of only $4H_2$-cluster and farH_2-$3H_2$cluster without considering the surface (COBN). In this case the total energy of $4H_2$-cluster is found to be more negative than the farH_2-$3H_2$cluster. This energy difference signifies that there is a contribution to the binding energy due to H_2-H_2 self-interaction along with the partial charge transfer from the surface to H_2 molecules. The results indicate that sharing of electrons of bonding orbitals of H_2 is the cause of this phenomenon. Our results hence suggest that, as the binding value is in the physisorption range here, the H_2-H_2 self-interaction energy also needs to be considered while computing the binding energies. The details of H_2 adsorption on the different surfaces and the various means used to explain the interaction are tabulated in Table 2.

3.5 Bond exchange mechanism

Here we investigate the possibility and limitation on hydrogenation of pure and doped *h-BN* monolayer and discuss how an external mediator can assist in the spillover of hydrogen atom via bond exchange mechanism. First we elaborately study the H_2 interaction with partially hydrogenated surfaces considering the surfaces are highly stable and can be realized.

It has been found that the H_2 binding with partially hydrogenated COBN surface is high compared to all the other surfaces discussed earlier. The optimized structures of H_2 molecule on partially hydrogenated COBN surface is shown in Fig. 6a. The binding energy value is -0.32 eV and the distance d_a is found to be 2.53 Å. Similar fact has also been observed for the case of partially hydrogenated, undoped *h-BN* surface.

In order to realize the hydrogenation, the first step is the dissociation of the H_2 molecule. On pure *h-BN* surface the energy required to dissociate the H_2 molecule into two H atoms is more than 2.29 eV, suggesting that dissociation at ordinary temperatures is quite unlikely. Similar fact has been observed on a pristine graphene surface, wherein the dissociation barrier for H_2 is quite high[30], but the dissociation of H_2 and hopping of H atom to the nearest carbon atom is feasible by using a metal cluster that acts as a catalyst and lowers the energy barrier (E_a) to about 0.65 eV.[57] However, in our case the doped COBN system is itself acting as a catalyst.[41] In order to calculate the dissociation barrier, we performed transition state search calculations considering a single H_2 molecule adsorbed on COBN surface as the initial state (I.S.) and two hydrogen atoms adsorbed on atop of boron atoms as the final state (F.S.), the structures of which are shown in the inset of Fig. 6b. Our calculations reveal that the energy required for the bond breaking of H_2 on COBN surface is about 0.78 eV, the transition state (T.S.) structure is shown in the inset of Fig. 6b. The reaction energy in this case is about -2.75 eV, indicating the high stability of H atom as compared to H_2 molecule on COBN surface. Also it has to be noted that the binding energy of the atomic hydrogen adsorbed on COBN is very high compared to that on pure *h-BN* system. These results clearly indicate that dissociation of H_2 on COBN surface is possible at low temperature, whereas on pure *h-BN* surface it needs very high temperature.

Now after dissociation, the migration of hydrogen atom with low energy barrier is required for easy and fast kinetics at low temperature to realize the hydrogenation of surface. Partially hydrogenated pure *h-BN* and COBN surfaces are considered for our purpose to find the migration energy barrier. First we discuss the case of H atom migration on pure *h-BN* surface. The I.S., F.S. and the T.S. structures are shown in the inset of Fig. 6c. In the inset of Fig. 6c (see the I.S. structure) the small bended red arrow is used to depict the H migration direction, pointing to one of the closest and unoccupied B atom on the surface from its I.S. The dragging of H atom from paired chair like site to the nearest B site needs very high barrier energy of about E_a = 2.35 eV. The reaction energy in this case is highly endothermic indicating that clustering of H atom is more favorable.[30] Similarly considering the COBN surface, the energy barrier to migrate the H atom is E_a = 3.05 eV (the energy barrier is defined as the energy of T.S. in reference to the energy of I.S, shown in Fig. 6d), which is higher than the pure hydrogenated case. In this case also the reaction energy is endothermic in nature. The corresponding T.S. structure is illustrated in the inset of Fig. 6d, in which the H atom is away from the boron sites with an average B-H distance of about 2.4 Å. The barrier energy in both the cases indicates an impractical migration of hydrogen atom at ambient condition. We also considered the single H migration just after the H_2 dissociation near the active site. For this case the barrier energy is about 2.32 eV (the I.S., F.S and the calculated barrier energy are demonstrated in the Fig. S6). It can be concluded from this study that although dissociation is possible in COBN surface, the migration of H atom by its own needs very high temperature (looks not viable).

To solve the problem for easy and fast migration of H atom at ambient conditions we proposed a new mechanism that can be termed as bond exchange mechanism using external catalysts or agents. Here we introduce two examples of external catalyst, borane (BH_3) and

gallane (GaH_3) molecules. A BH_3 molecule near to one of the dissociated H atoms adsorbed on COBN surface is considered as I.S. (completely relaxed structure) and a BH_3 molecule on close proximity with a H atom adsorbed on a neighboring B atom has been considered as F.S. (structures are shown in the insets of Fig. 6e). So here we introduce bond exchange spillover mechanism i.e. H atom exchange at the same ring via migration of H atom using bond breaking (from surface) and swapping of one of the H atom of BH_3 to the surface, this is clearly seen from the structure of I.S. and F.S. In a sense, the H atom (neutral form) spillover through secondary catalyst via bond exchange is similar to the Grotthus-proton exchange in the water network.[39, 58] The bond exchange barrier energy to migrate the H atom using BH_3 molecule is about E_a = 0.57 eV, which is very low compared to the energy required to desorb BH_4 by breaking the surface-H bond far from the COBN surface (about 2.56 eV). The reaction energy is about 0.38 eV, indicating the route is slightly endothermic in nature. This is an obvious fact, as during bond exchange spillover, the H atom is moving away from the active site. It is also worth noting that while BH_3 interacts quite strongly with a H atom that is adsorbed near to the doping site, the interaction energy of BH_3 is not so strong with a H atom adsorbed far from the dopant site. Hence we can infer that the complete dissociation of BH_4 is less favorable compared to the H atom migration using bond exchange mechanism. Similar results have been observed by considering GaH_3 as a secondary catalyst. The structures of reaction states (I.S., F.S. and T.S.) to explain the bond exchange mechanism using the GaH_3 as secondary catalyst on hydrogenated COBN surface are shown in the inset of Fig. 6f. In this case the maximum energy required for the bond exchange is about E_a = 0.65 eV and the reaction energy is about 0.35 eV. Hence the bond exchange mechanism sufficiently decreases the activation barrier (E_a < 0.65 eV) for H migration on the substrate. We also considered NH_3 and SiH_4 as secondary catalysts, but found them not to be suitable candidates to initiate bond exchange spillover (see Fig. S7).

4 Conclusions

In summary, first principles theory based DFT calculations explain significantly the increased binding strength for H_2 molecule with *n*-doped *h-BN* surface compared to the pristine form. To find out the best storage medium, we checked various types of *h-BN* nanostructures and finalize that some particular systems like COBN, 2COBN, $2COB_{10}N_{11}$ nanocage and partially hydrogenated COBN surfaces are superior media for the purpose. It has been observed that electron donation from the surface donor state to the $1\sigma^*$ orbital of the H_2 molecule, is the governing reason for the stronger binding. The 6.25 % C-O doping is enough to store 7.4 wt % of H_2 which is quite acceptable according to DOE target. On COBN surface the barrier energy to split the H-H bond is estimated to be about 0.78 eV. But the spillover of H atom needs very high temperature, which seems quite unfeasible for the hydrogenation of such surface. We proposed that easy H atom migration along the surface is possible via bond exchange mechanism using some external mediators (ex: GaH_3, BH_3). The hydrogen atom can migrate via bond exchange mechanism in the same hexagonal ring with energy barrier of about 0.57- 0.65 eV. Also it has been found that the partial hydrogenation on the surfaces can enhance the binding of molecular hydrogen. Our findings conclude that metal free light element based C and O doped *h-BN* nanostructure is an efficient medium to store hydrogen energy and the bond exchange mechanism can be used as an effective approach for adsorption and desorption of hydrogen atoms.

Acknowledgements

RT and SS thanks Science and Engineering Research Board (SERB), India for the financial support (Grant no: SB/FTP/PS028/2013). All authors thank SRM Research Institute, SRM University for providing supercomputing facility and financial support.

Supplementary Information

H_2 molecule interaction with additional doped surfaces and also the case of higher doping percentage has been considered. Explain the possibility of bond exchange mechanism using ammonia (NH_3) and silane (SiH_4) molecules as an external mediator.

References

1 S. Patchkovskii, J. S. Tse, S. N. Yurchenko, L. Zhechkov, T. Heine, G. Seifert, *Proc. Natl. Acad. Sci. U. S. A.*, 2005, **102**, 10439−10444.

2 H. Si, L. J. Peng, J. R. Morris, B. C. Pan, *J. Phys. Chem. C*, 2011, **115**, 9053–9058.

3 R. E. Barajas-Barraza, R. A. Guirado-López, *Phys. Rev. B*, 2002, **66,** 155426.

4 P. O. Krasnov, F. Ding, A. K. Singh, B. I. Yakobson, *J. Phys. Chem. C*, 2007, **111**, 17977−17980.

5 F. H. Yang, R. T. Yang, *Carbon*, 2002, **40**, 437−444.

6 E. Yoo, L. Gao, T. Komatsu, N. Yagai, K. Arai, T. Yamazaki, K. Matsuishi, T. Matsumoto, J. Nakamura, *J. Phys. Chem. B*, 2004, **108**, 18903−18907.

7 Y. Guo, K. Jiang, B. Xu, Y. Xia, J. Yin, Z. Liu, *J. Phys. Chem. C*, 2012, **116**, 13837−13841.

8 D. Sen, R. Thapa, K. K. Chattopadhyay, *Int. J. Hydrogen Energy*. 2013, **38**, 3041−3049.

9 W. H. Shin, S. H. Yang, W. A. Goddard, J. K. Kang, *Appl. Phys. Lett*., 2006, **88**, 053111.

10 A. Sigal, M. I. Rojas, E. P. M. Leiva, *Int. J. Hydrogen Energy*., 2011, **36**, 3537−3546.

11 H-L. Park, Y-C. Chung, *Comp Mater Sci*., 2010, **49**, S297−S301.

12 T. Yildirim, S. Ciraci, *Phys. Rev. Lett*., 2005, **94**, 175501.

13 P. Chen, Z. Xiong, J. Luo, J. Lin, K. L. Tan, *Nature*, 2002, **420**, 302–304.

14 L. Zhou, *Renv*. *Sust. Energ. Rev.*, 2005, **9**, 395–408.

15 Y. Ma, Y. Xia, M. Zhao, R. Wang, L. Mei, *Phys. Rev. B*, 2001, **63**, 115422.

16 Y-H. Kim, Y. Zhao, A. Williamson, M. J. Heben, S. B. Zhang, *Phys. Rev. Lett.*, 2006, **96**, 016102.

17 R. C. Lochan, M. Head-Gordon, *Phys. Chem. Chem. Phys.*, 2006, **8**, 1357–1370.

18 Z. Zhang, K. Cho, *Phys. Rev. B* 2001, **75**, 075420.

19 M. Sankaran, B. Viswanathan, Carbon 2006, **44**, 2816–2821.

20 M. Suri, M. Dornfeld, E. Ganz, *J. Chem. Phys.* 2012, **116**, 3661–3666.

21 L. J. Murray, M. Dincă, J. R. Long, *Chem. Soc. Rev*., 2009, **38**, 1294−1314.

22 C. Chen, J. Zhang, B. Zhang, H. M. Duan, *J. Phys. Chem. C*, 2013, **117**, 4337−4344.

23 G. Kim, S-H. Jhi, S. Lim, N. Park, *Phys. Rev. B*, 2009, **79**, 155437.

24 E. Durgun, Y-R. Jang, S. Ciraci, *Phys. Rev. B*, 2007, **76**, 073413

25 X. Wu, J. L. Yang, X. C. Zeng, *J. Chem. Phys.*, 2006, **125**, 044704.

26 Md. Shahzad Khan, M. Shahid Khan, *Int. Nano. Lett*., 2011, **1**, 103−110.

27 M. Chen, Y-J. Zhao, J-H. Liao, X-B. Yang, *Phys. Rev. B*, 2012, **86**, 045459.

28 H. Y. Wu, X. F. Fan, J-L. Kuo, W-Q. Deng, *Chem. Commun.*, 2010, **46**, 883−885.

29 Y. Wang, F. Wang, B. Xu, J. Zhang, Q. Sun, Y. Jia, *J. Appl. Phys*., 2013, **113**, 064309.

30 S. S. Han, H. Jung, D. H. Jung, S-H. Choi, N. Park, *Phys. Rev. B*, 2012, **85**, 155408.

31 M. D. Segall, P. J. D. Lindan, M. J. Probert, C. J. Pickard, P. J. Hasnip, S. J. Clark, M. C. Payne, *J. Phys. Condens. Matter.*, 2002**, 14**, 2717−2744.

32 G. Kresse, J. Furthmüller, *Comput. Mat. Sci.*, 1996, **6**, 15-50.

33 J. P. Perdew, K. Burke, M. Ernzerhof, *Phys. Rev. Lett.*, 1996, **77**, 3865−3868.

34 Y. Wang, J. P. Perdew, *Phys. Rev. B*, 1991, **44**, 13298.

35 D. Vanderbilt, *Phys. Rev. B*, 1990**, 41**, 7892−7895.

36 P. E. Blöchl, *Phys. Rev. B* 1994**, 50**, 17953-17979.

37 A. Tkatchenko, M. Scheffler, *Phys. Rev. Lett.*, 2009**, 102**, 073005.

38 F. Ortmann, F. Bechstedt, W.G. Schmidt, *Phys. Rev. B*, 2006, **73**, 205101.

39 R. Thapa, N. Park, *J. Phys. Chem. Lett*., 2012, **3**, 3065−3069.

40 O. L. Krivanek, M. F. Chisholm, V. Nicolosi, T. J. Pennycook, G. J. Corbin, N. Dellby, M. F. Murfitt, C. S. Own, Z. S. Szilagyi1, M. P. Oxley, S. T. Pantelides, S. J. Pennycook, *Nature*, 2010**, 464**, 571−574.

41 S. Sinthika, E. Mathan Kumar, R. Thapa, *J. Mater. Chem. A*, 2014, **32**, 12812−12820.

42 V. Tozzini. V. Pellegrini, *Phys. Chem. Chem. Phys.*, 2013, **15**, 80−89.

43 D. Jiang, Z. Chen, Graphene Chemistry Theoretical Perspectives. 1st edn 382.

44 W. Lei, H. Zhang, Y. Wu, B. Zhang, D. Liu, S. Qin, Z. Liu, L. Liu, Y. Ma, Y. Chen, *Nano Energy*, 2014, **6,** 219-224.

45 Y. Y. Sun, K. Lee, L. Wang, Y-H. Kim, W. Chen, Z. Chen, S. B. Zhang, *Phys. Rev. B*, 2010, **82**, 073401.

46 J. Wang, J. Li, S-S. Li, Y. Liu, *J. Appl. Phys*., 2013, **114**, 124309.

47 Z. M. Ao, Q. Jiang, R. Q. Zhang, T. T. Tan, S. Li, *J. Appl. Phys.*, 2009, **105**, 074307.

48 K. Ulman, D. Bhaumik, B. C. Wood, S. Narasimhan, *J. Chem. Phys*., 2014, **140**, 174708.

49 Q. Sun, Q. Wang, P. Jena, Y. Kawazoe, *J. Am. Chem. Soc*., 2005, **127**, 14582−14583.

50 S-H. Jhi, G. Kim, N. Park, *J. Kor. Phys. Soc.*, 2008**, 52**, 1217−1220.

51 S. Banerjee, C. G. S. Pillai, C. Majumder, *Appl. Phys. Lett*., 2013, **102**, 073901.

52 N. Song, Y. Wang, Q. Sun, Y. Jia, *Appl. Surf. Sci*., 2012, **263**, 182–186.

53 J. Zhou, Q. Wang, Q. Sun, P. Jena, X. S. Chen, *Proc. Natl. Acad. Sci. U. S. A.*, 2010, **107**, 2801-2806.

54 W. An, X. Wu, J. L. Yang, X. C. Zeng, *J. Phys. Chem. C*, 2007, **111**, 14105-14112.

55 M. Yoon, S. Yang, E. Wang, Z. Zhang, *Nano Lett*., 2007, **7**, 2578-2583.

56 Q. Sun, P. Jena, Q. Wang, M. Marquez, *J. Am. Chem. Soc*., 2006, **128**, 9741-9745.

57 H-F.Wu, X. Fan, J-L. Kuo, W-Q. Deng, *J. Phys. Chem. C*, 2011, **115**, 9241–9249.

58 Y. Zhao, T. Gennett, *Phys. Rev. Lett.*, 2014**, 112**, 076101.

System	$E_{B.E}$(PBE)	$E_{B.E}$(PBE+TS)	$E_{B.E}$(PW91)	$E_{B.E}$(PW91+OBS)	$E_{B.E}$(PBE_{sol})
h-BN	+0.04	-0.04	+0.01	-0.15	+0.01
C-*h-BN*	+0.01	-0.06	-0.02	-0.16	-0.01
O-*h-BN*	+0.04	-0.06	-0.04	-0.18	+0.01
CO-*h-BN*	-0.05	-0.16	-0.045	-0.28	-0.11
2C-*h-BN*	+0.11	-0.06	-0.033	-0.17	-0.01
2CO-*h-BN*	-0.008	-0.09	-0.013	-0.21	-0.05

Table 1. Binding energies ($E_{B.E}$) of single H_2 adsorbed on different surfaces are calculated using various exchange and correlation functional. Gray color shading indicates the highest binding of H_2 with C and O co-doped *h-BN* surface compare to other systems. All the energy values are in eV.

System	Functional	$E_{B.E}$ (eV)	Wt%	d_a (Å)	d_b (Å)	Interaction
Metal as adsorbent						
Mg doped Graphene oxide[22]	PBE	0.38	5.6	2.4	0.79	Charges transfer from H_2 to the metal ions, polarization and kubas interaction
Mg and Ca doped graphene complexes[23]	LDA & GGA	0.31(0.21)	6.2	2.66	0.76	Kubas and multipole Coulomb interaction
Be substituted SWNT[24]	GGA	0.40	2.4	2.0	0.77	Charge transfer from Be to nearest carbon atom
Platinum doped BNNT[25]	PBE	0.365	4-8	1.88	0.82	Charge transfer from surface to H_2 and polarization interaction
Aluminum doped graphene[47]	LDA	0.260	5.13	2.7	–	High charge transfer from Al to H_2
Clustering of Ti on C_{60} surface[49]	PW91	0.38	2.85	–	0.75	Charge polarization interaction
Sc or Ti decorated on B doped fragmented graphitic shells (FGS)[50]	LDA and GGA	0.3-0.5	4-8	–	–	Charge transfer and Coulomb interaction
Metallo-carbohedrenes(M_8C_{12}) (M=Ti, Sc and V)[51]	PBE	0.15-0.46	10.96-15.06	–	–	Charge transfer from metal to H_2
Ti(Sc) decorated boron-carbon-nitride sheet[52]	GGA	0.13-0.56	7.6-7.8	1.85 (2.21)	0.91 (0.78)	Kubas and polarization interaction
Low-elements as adsorbent						
BN sheet[53]	BLYP	0.14	7.5	–	0.74	Electric field induces polarization interaction
BNNT(stone-Wales defect)[54]	PBE	0.017	–	–	0.74	Charge transfer from defect site to H_2
Charged fullerene {C_{28}^{3+} & C_{82}^{6+}}[55]	LDA	0.32	8.0	–	–	Charge transfer from metal atom and polarization interaction due to electric field
{$Li_{12}C_{60}$}[56]	PW91	0.075	9.0	2.07	0.75	Polarization interaction
COBN surface (Current Study)	*PW91+OBS*	*0.28*	*7.4*	*2.58*	*0.78*	*Charge transfer from donor state of the substrate to $1\sigma^*$ orbital of H_2 molecule*
$2COB_{10}N_{11}$ (Current Study)	*PW91+OBS*	*0.16*	*7.36*	*2.41*	*0.76*	
Partially hydrogenated COBN (Current Study)	*PW91+OBS*	*0.32*	*7.3*	*2.53*	*0.75*	

Table 2. Bond lengths between H_2-surface (d_a) and H-H (d_b), exchange and correctional functional used, binding energy ($E_{B.E}$), weight percentage, storage mechanisms during the H_2 adsorption on different classes of materials.

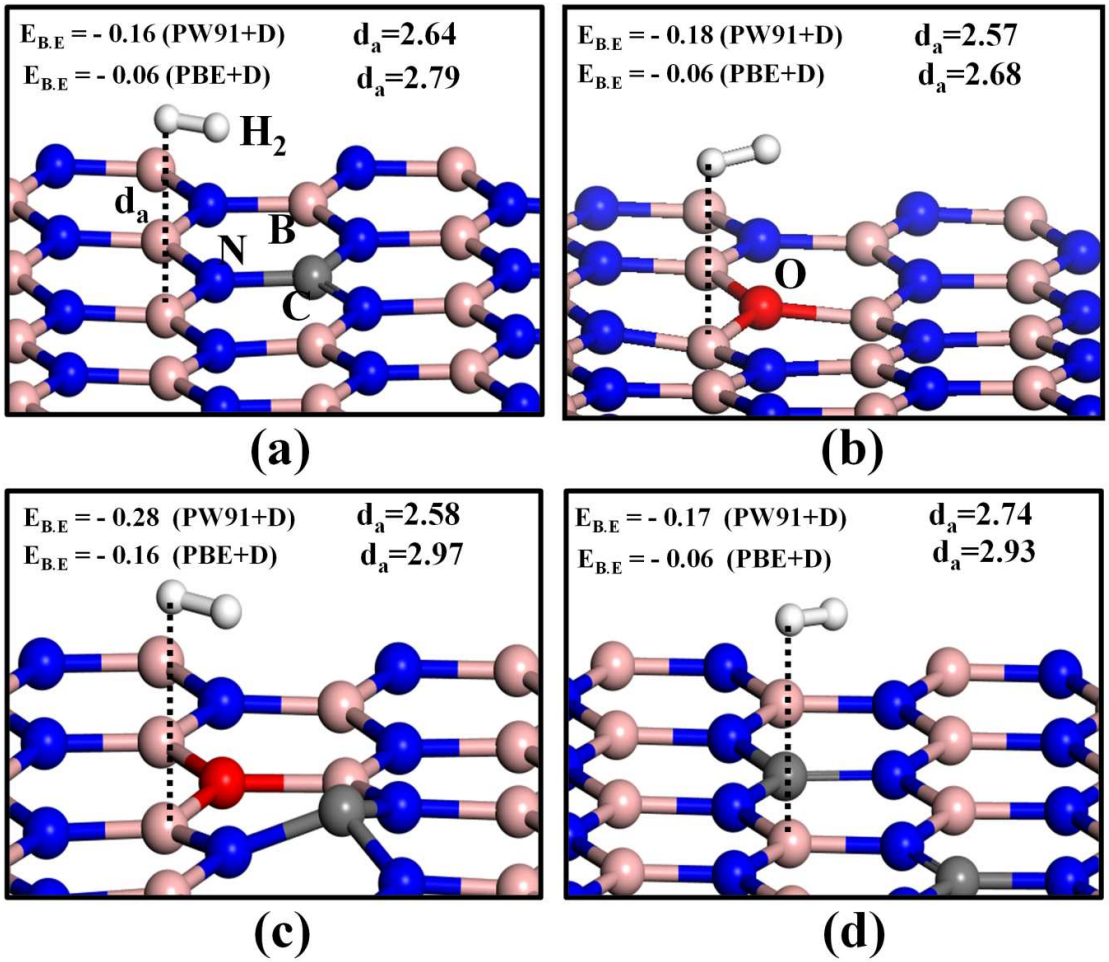

Fig. 1. Optimized geometries for single H_2 adsorption on (a) CBN (b) OBN (c) COBN and (d) 2CBN sheets. The red, gray, pink and blue balls represent the oxygen, carbon, boron, nitrogen atoms. Hydrogen molecule is represented by white balls. Binding energies ($E_{B.E}$) are in eV and are calculated using two different functional. H_2-surface distance (d_a) are in Å. Black dotted line is for guide to the eye to show nearest active sites.

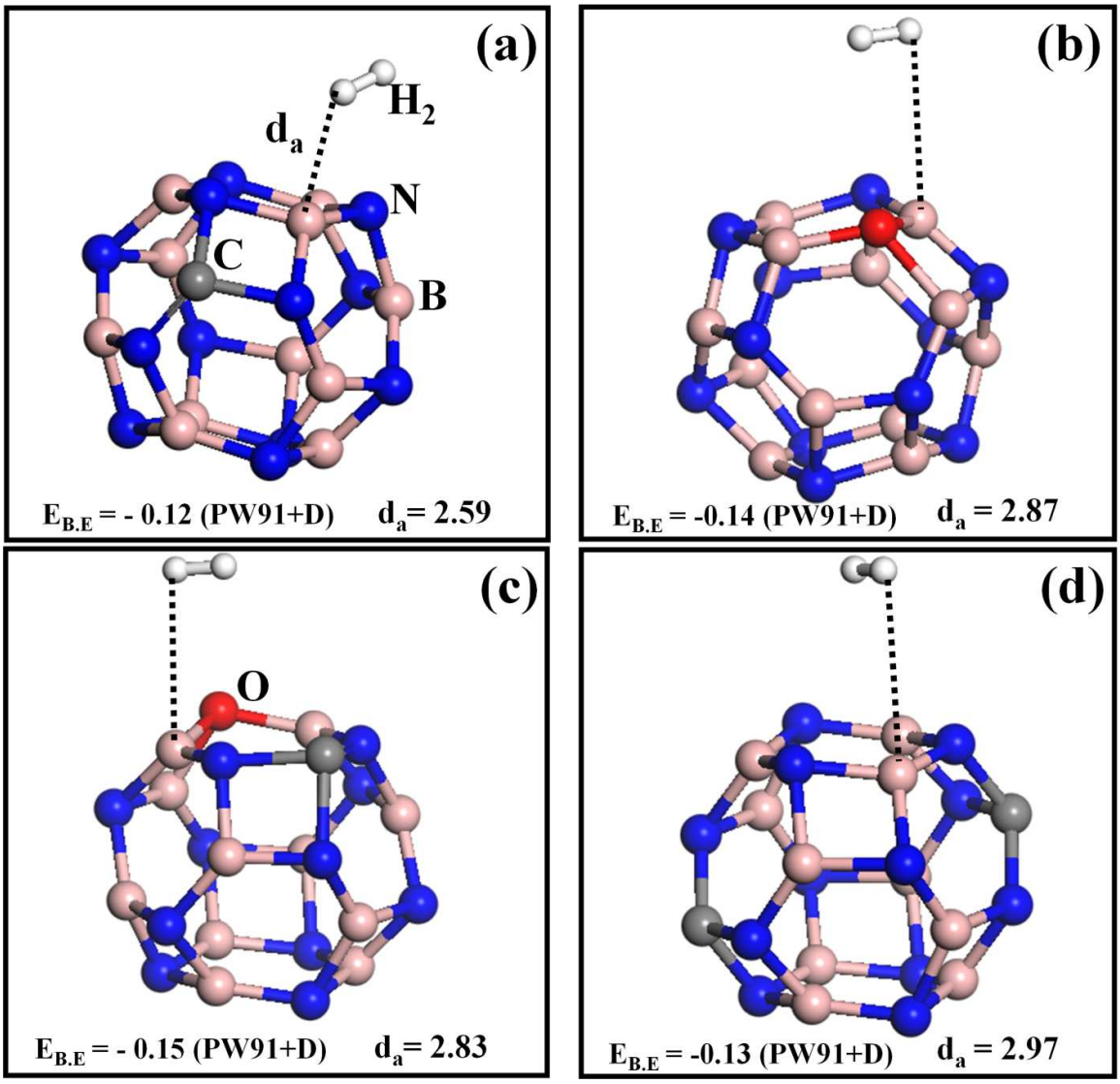

Fig. 2. Single H_2 molecule adsorption on different doped $B_{12}N_{12}$ nanocages (a) $CB_{11}N_{12}$, (b) $OB_{12}N_{11}$, (c) $COB_{11}N_{11}$, (d) $2CB_{10}N_{12}$. All colors and symbols follow the same convention as those used in Fig.1. Binding energies ($E_{B.E}$) are in eV and H_2-surface distance (d_a) are in Å.

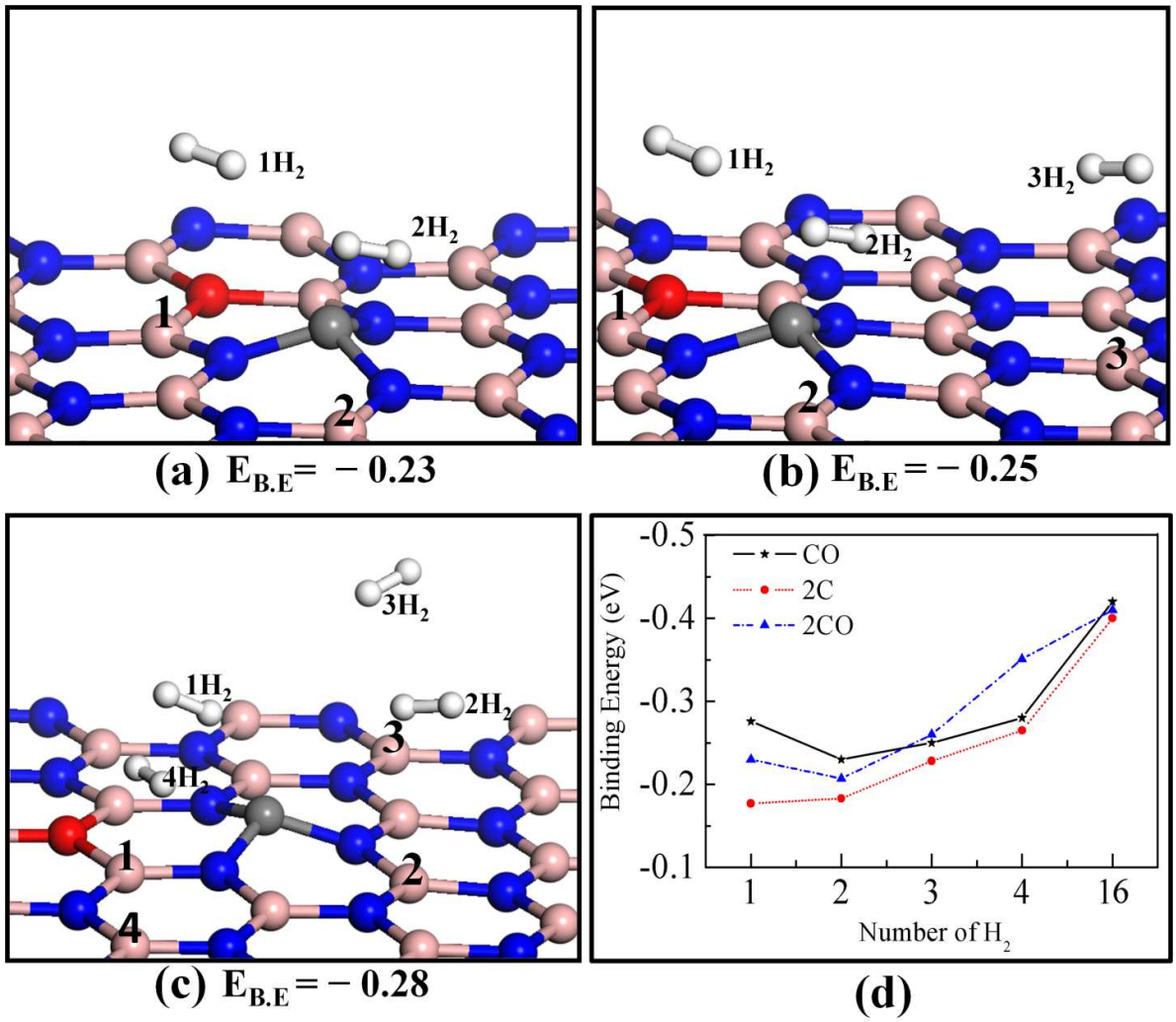

Fig. 3. Optimized structures for (a) two (b) three and (c) four hydrogen molecules adsorbed on COBN monolayer. The numbers preceding each H_2 represent the order in which H_2 is added and the numbers on the surface denote the corresponding adsorption site of each molecule. (d) Graph demonstrates the binding energy as function of number of H_2 molecules dsorbed on different surfaces. Binding energies ($E_{B.E}$) are in eV.

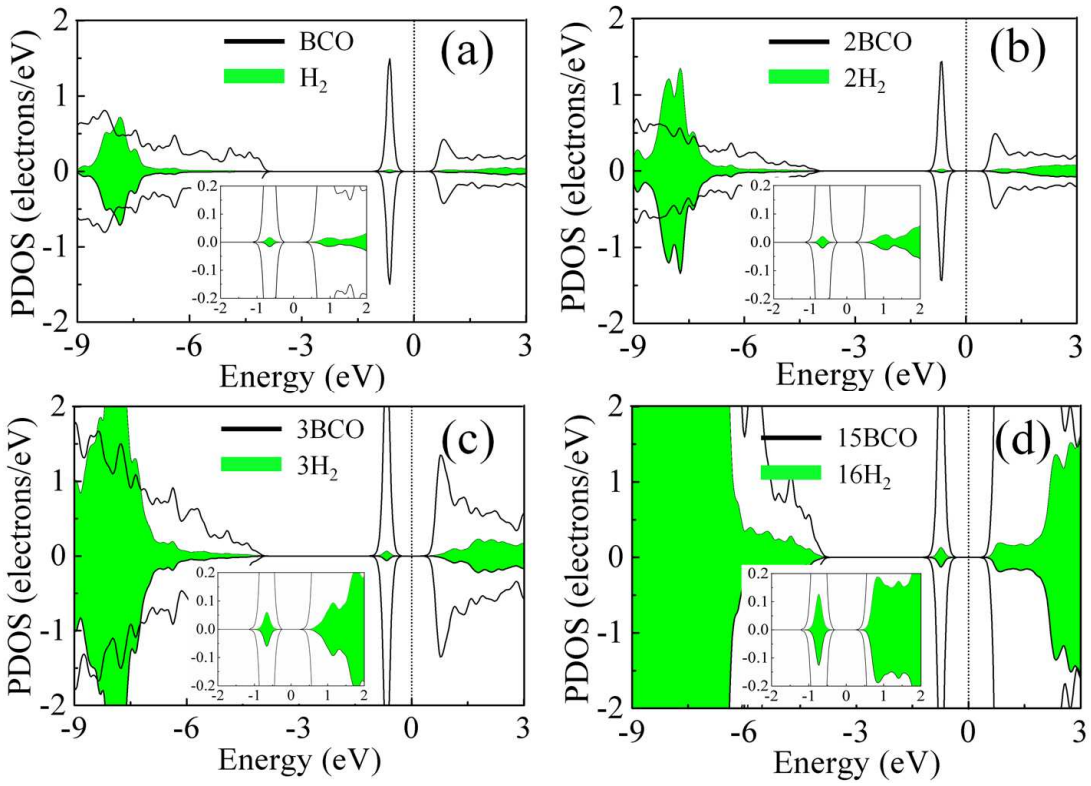

Fig. 4. Partial density of states of the H_2 molecules and the C, O and B atoms (adsorb sites) of (a) single H_2 molecule adsorption on COBN system, (b) two H_2 adsorption on COBN, (C) three H_2 adsorption on COBN and (d) 16 H_2 adsorption on COBN. The insets are magnified view of PDOS near the Fermi level.

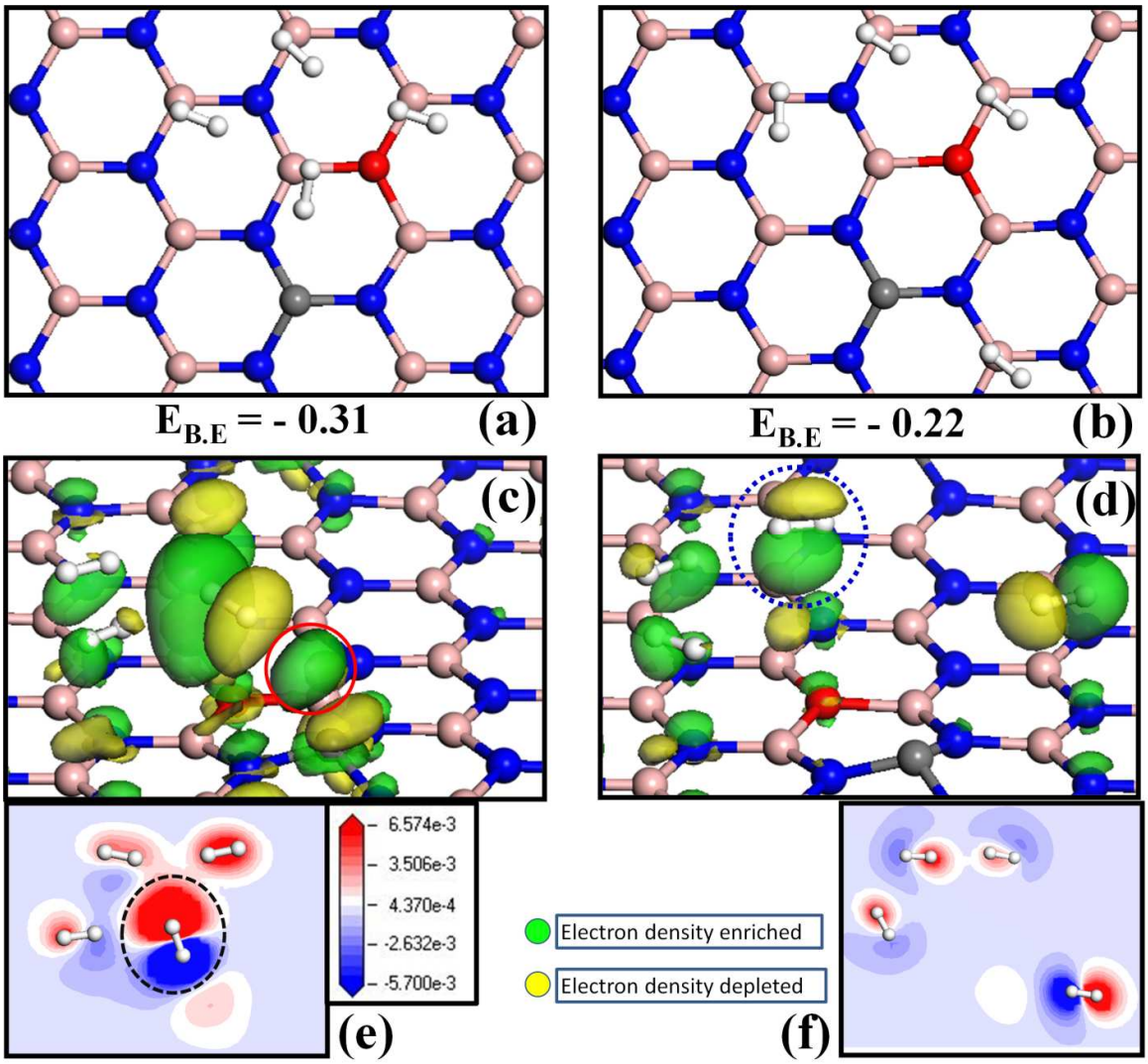

Fig. 5. Energy values and optimized structures of (a) $4H_2$ cluster, (b) $farH_2$-$3H_2$ cluster on COBN surface. Redistribution of electronic charge upon adsorption of (c) $4H_2$ cluster, (d) $farH_2$-$3H_2$ cluster on COBN surface. Green and yellow lobes correspond to a gain and depletion of electronic charge, respectively. The isosurfaces value 2×10^{-3} electrons/bohr is consider for all the cases. Charge density difference value is same for the two cases, a slice along the direction parallel to the COBN surface touches all the four H_2 molecules are demonstrate in (e) & (f). Gain of electron is indicated by red color, loss of electron is shown by blue color and white color indicates the region with very small change in the electron density. Binding energies ($E_{B.E}$) are in eV.

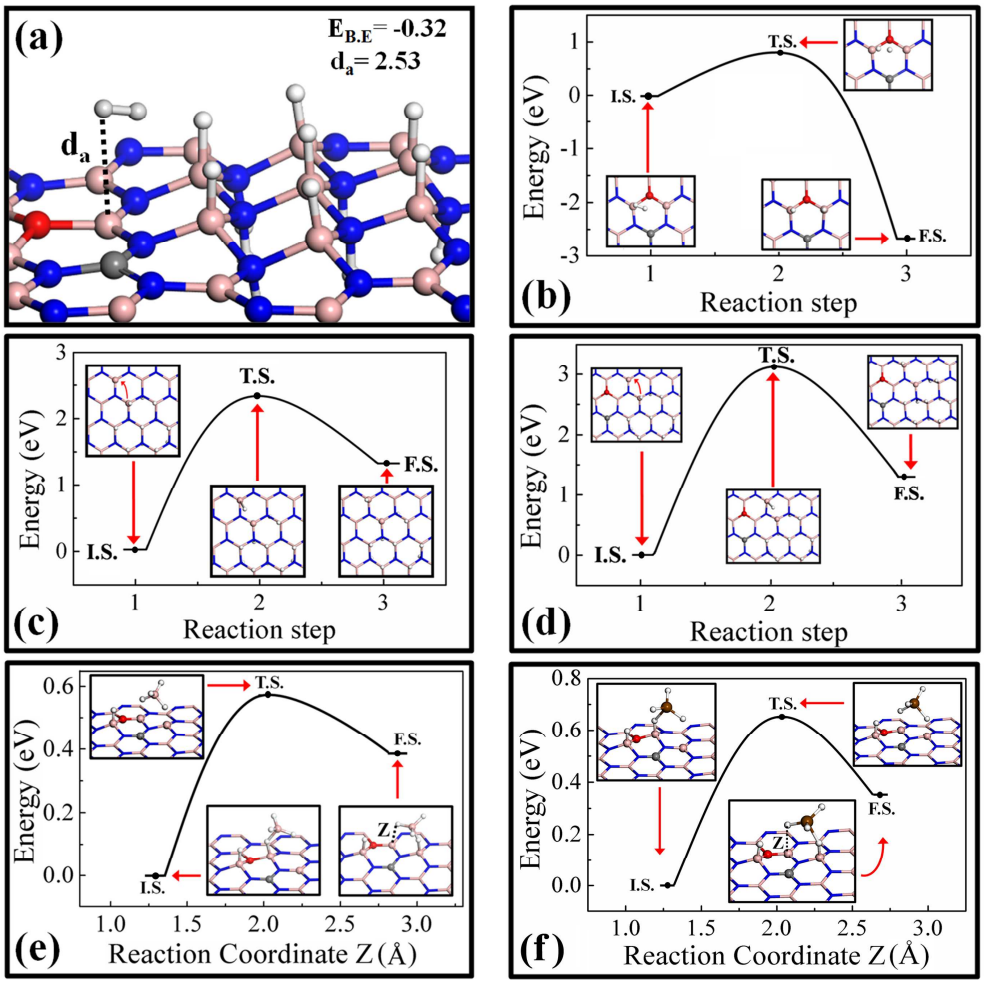

Fig. 6 Optimized structure for (a) H_2 adsorption on partially hydrogenated COBN surface. The binding energy (eV) and H_2-surface distance (Å) are written in the inset; (b) shows the barrier energy for the dissociation of H_2 on COBN surface. The barrier energy curve during the migration of H atom from the paired configuration on pure *h-BN* and COBN surfaces are shown in (c) and (d) respectively. The energy barrier curve during the hydrogen spillover on COBN surface via bond exchange mechanism using secondary mediator BH_3 and GaH_3 are shown in (e) and (f) respectively. In (b) to (f) the inset shows the relaxed structure of initial state (I.S.), transition state (T.S.) and final state (F.S.). The black line connecting I.S., T.S. and F.S. are only for guide to the eye.

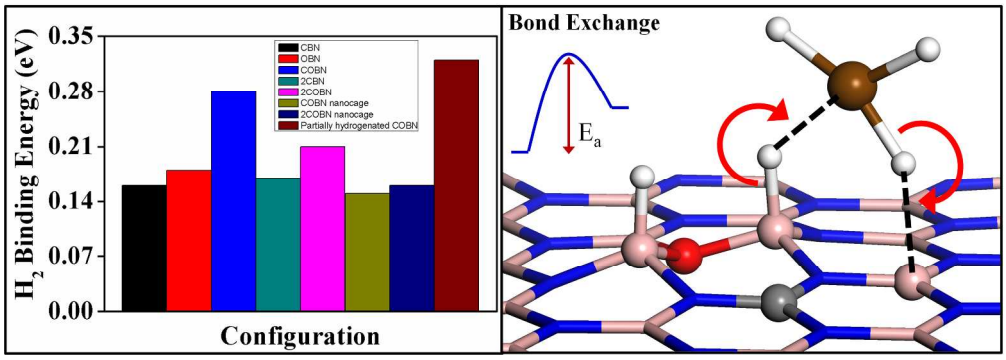

Metal free surface for H2 storage: Bond exchange mechanism
738x259mm (96 x 96 DPI)